Materials Science & Engineering A 723 (2018) 70–78

Contents lists available at ScienceDirect

Materials Science & Engineering A

journal homepage: www.elsevier.com/locate/msea

Refinement of Mg alloys crystal structure via Nb-based heterogeneous substrates for improved performances

L. Bolzoni[a,b,*], U. Joshi[b], R. Alain[c], D. Garetto[d], N. Hari Babu[b]

[a] Waikato Centre for Advanced Materials, School of Engineering, The University of Waikato, Private Bag 3105, Hamilton 3240, New Zealand
[b] Brunel University London, Institute of Materials and Manufacturing, Kingston Lane, Uxbridge, Middlesex UB8 3PH, United Kingdom
[c] Consultan Innovation, 8 rue de la victoire, 69160 Tassin La Demi-Lune, France
[d] Brabant Alucast International, S&D Office Torino, C.so Turati 13/A, 10141 Torino, Italy

ARTICLE INFO

Keywords:
Magnesium alloys
Casting methods
Grains and interfaces
Grain refinement
Mechanical behaviour

ABSTRACT

Lightness and high specific strength make magnesium alloys ideal materials for the transportation industry, especially the automotive sector that is struggling to cope with the everyday more stringent regulations on emission of carbon dioxide. Wrought magnesium alloys are difficult to deform because of the few active slip systems characteristic of their hexagonal close-packed lattice. Consequently, most of the commercially available magnesium alloys are alloys based on the Mg-Al binary system used in casting processes. The improvement of the mechanical properties of these alloys cannot be achieved by means of grain refinement using Zr due to the formation of Zr aluminides. In this study we propose a novel chemical composition that can refine all types of Mg alloys as proved in the Al-containing AM50 Mg alloy. We demonstrate that Nb-B inoculation of Mg alloys promotes the formation of heterogeneously nucleated primary α-Mg grains leading to the reduction of the grain size and this is obtained over a wide range of cooling rates. We also show that the grain refinement achieved leads to the improvement of the properties of high pressure die cast Mg automotive components and has the potential to enhance the mechanical properties of cast Mg alloys.

1. Introduction

The interest for Mg as structural metal has increased in recent years [1] because of some of its physical, mechanical and technological characteristics such as low density (i.e. the lowest among metals, apart Be), good damping behaviour, strength and stiffness as well as good castability and machinability [2]. The automotive industry is very much interested in the lightweighting related to the use of Mg and has, up to date, driven most of the developments [3–6] which were focused on (die) casting because Mg has poor workability as result of its hexagonal close-packed (H.C.P.) crystal structure [7]. Mg alloys are generally divided on the basis of the presence of Al as major alloying elements; consequently, Al-free and Al-containing Mg alloys are available. The latter are preferred because of their low cost and good castability [4]. Among them, the Mg-9Al-1Zn (AZ91) and Mg-3Al-1Zn (AZ31) as well as Mg-6Al-0.5Mn (AM60) and Mg-5Al-0.5Mn (AM50) alloys are the most widely studied and employed [2]. The great majority of Mg industrial castings are obtained by means of the cold chamber high pressure die casting (HPDC) process. Mg is characterised by a hexagonal lattice structure with few slip systems and, thus, by a large Taylor factor [8]. Therefore, the refinement of Mg alloys microstructure is vital to improve their characteristics, especially in terms of mechanical performances. It has been proven that good combinations of strength/ductility are possible in fine-grained Mg alloys [9].

As per the classical nucleation theory, fine grain structures in cast Mg alloys can be achieved when using (very) fast cooling rates. Inoculation, i.e. the addition of heterogeneous nucleation substrates with appropriate features which lower the energy needed for the nucleation of primary α-Mg grains, is another way to refine the microstructure (grain refinement). To efficiently promote grain refinement, the heterogeneous substrates should have low contact angle (good wettability), good lattice match and, possibly, similar crystal structure as well as good thermal stability to prevent their dissolution in the molten metal and/or their interaction with the alloying elements. Zr is considered the most effective grain refiner for Mg because they share the same H.C.P. crystal structure with compatible lattice parameters [10] and because Zr has a high growth restriction factor on Mg [11]. Nonetheless, Zr is not effective at all for the refinement of Al-containing Mg alloys [12] because it has a great affinity and reacts with Al, to form Zr aluminides, inhibiting its role as heterogeneous nucleation substrate. This is due to the fact that the superficial layer of Zr aluminide formed on top of Zr particles does not possess a sufficiently low lattice

* Corresponding author at: Waikato Centre for Advanced Materials, School of Engineering, The University of Waikato, Private Bag 3105, Hamilton 3240, New Zealand.
E-mail address: leandro.bolzoni@gmail.com (L. Bolzoni).

https://doi.org/10.1016/j.msea.2018.03.005
Received 15 January 2018; Received in revised form 28 February 2018; Accepted 2 March 2018
Available online 06 March 2018

mismatch as to promote the nucleation of primary α-Mg grains [13]. Different alternative methods for the refinement of Al-containing Mg alloys are available in the current literature among which melt treatments (superheating [14], Elfinal process [15], melt agitation [16]), inoculation with carbon [6] or addition of solute elements (Ca, Sr or rare earths) [17]. Nevertheless, each and every one of these solutions has some remarkable issue of efficiency and/or reliability and a consistent and easy to apply refiner for Al-containing Mg alloys is still missing in commercial use [12]. The reader is referred to the review of Ali et al. [13] for a full account of the current research progress in grain refinement of cast magnesium alloys.

The aim of this work is to propose an alternative composition to refine the microstructure of Mg alloy, independently of whether they contain Al or not, studying the inoculation of the AM50 alloy by means of Nb-based heterogeneous substrates (i.e. Nb-B inoculation). Our study demonstrates that consistent grain refinement of Mg alloys is possible via Nb-B inoculation, which is effective over a great range of cooling conditions. The reduction of the grain size leads to the improvement of the deformability of high pressure die cast parts for the automotive industry. A higher improvement of the mechanical performances is also forecast in Mg alloys solidified using casting processes characterised by slower cooling rates such as die pressure or sand casting.

2. Experimental procedure

2.1. Starting materials

Grain refinement experiments were performed on a commercial AM50 Mg alloy (Al = 5 wt%, Mn = 0.5 wt%, Zn + Si + Cu + Fe + Ni < 0.35 wt% and Mg = base). Generally, the alloy was melted inside steel crucibles under a constant flow of SF_6 + N_2 protective atmosphere in combination with the addition of an Al-Be master alloy to prevent burning of the material. The melting temperature for both the reference and the inoculated materials was set to 10 °C higher than the pouring temperature (i.e. 690 ± 3 °C). Nb-B inoculation of the melt was carried out by means of an Al-Nb-B master alloy [18,19]. Addition level and contact time were set to 0.1 wt% of master alloy and 30 min, respectively.

2.2. Grain refinement experiments

The grain refining efficacy of Nb-B inoculation was assessed at lab scale using different moulds with simple geometry to simulate diverse industrial casting processes. In particular, a copper mould (cooling rate range: 5–150 °C/s) and cold chamber HPDC samples/components (cooling rate ~ hundreds of °C/s) were analysed. Grain size was measured as per ASTM E:112 (intercept linear method) using light polarised micrographs taken on polished and etched samples. Mechanical properties were obtained either from standard cylindrical (6.35 mm) and flat samples (5 mm) tensile samples or flat (2 and 3 mm) bending specimens shown in Fig. 1. All of the samples for mechanical characterisation were manufactured by HPDC that is one of the most common casting methods for Mg alloys. The HPDC parameters used were: injection temperature 690 °C, die temperature 180 °C, dwell time 9 s, injection speed 6.5 m/s and amount of lubricant 2%. It is worth mentioning that, for consistency, the set of parameters was kept constant when comparing the AM50 Mg alloy without and with Nb-B inoculation.

2.3. Proof of the concept for industrial production

Based on the results of the characterisation of the samples made at lab scale, the reliability of the methodology developed was tested by manufacturing, in an industrial environment, actual automotive components made out of the AM50 alloy without and with Nb-B inoculation and testing their deflection to failure.

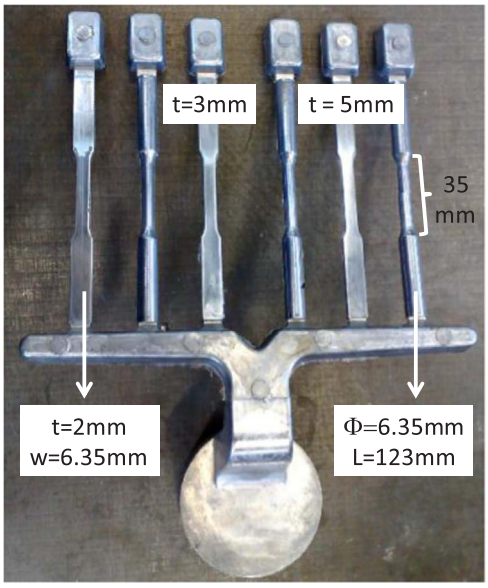

Fig. 1. Geometry and dimensions of the high pressure die casting samples used to measure the mechanical properties. Note: 6.35 mm cylindrical and 5 mm flat samples were tested under quasi-static tensile conditions and 2 mm and 3 mm flat specimens were tested to bending.

3. Results

3.1. Grain refinement experiments

Fig. 2 shows representative example of the refinement of the grain structure of the AM50 alloy by Nb-B inoculation. Macroetched surfaces and light polarised micrographs along with the predicted variation of the grain size versus the cooling rate are shown. The inoculation of the starting material does not change the morphology of the primary α-Mg grains because both materials are characterised by equiaxed dendritic crystals. As expected, the grain size of the reference alloy decreases along with the increment of the cooling rate. As per the standard nucleation theory, the higher the heat extraction rate, the shorter the time for grain growth, and the finer the resulting microstructure. Inoculation induces a refinement of the size of the primary α-Mg grains independently of the cooling conditions although its effect becomes less prominent with the decreasing of the solidification time (i.e. higher cooling rates).

3.2. Mechanical properties of high pressure die cast samples

Figs. 3 and 4 show a summary of the tensile and bending performances, respectively, of the standardised samples produced by HPDC.

From Fig. 3(a) it can be seen that the yield strength of the AM50 alloy without and with Nb-B inoculation are comparable among themselves regardless whether round 6.35 mm or flat 5 mm samples are considered. The most relevant point, in both cases, is the lower scattering of the data after the inoculation of the material. In the case of the ultimate tensile strength (Fig. 3(b)), the inoculation of the AM50 alloy leads to a general increment of approximately 3% of this properties (i.e. shift to the right) as well as reduction of the variability in both round and flat specimens. The same kind of behaviour is obtained in the case of the elongation (Fig. 3(c)) where the total improvement is greater than 11%. All the probability plots (Fig. 3(a)–(c)) show a rather linear trend due to the stochastic nature of the solidification process. The actual enhancements of the tensile performances in terms of absolute mean values as well as the reduction of their variation after inoculation are displayed in Fig. 3(d) and they are 0.5%, 3.0% and 11.2% for yield strength, ultimate tensile strength and elongation, respectively.

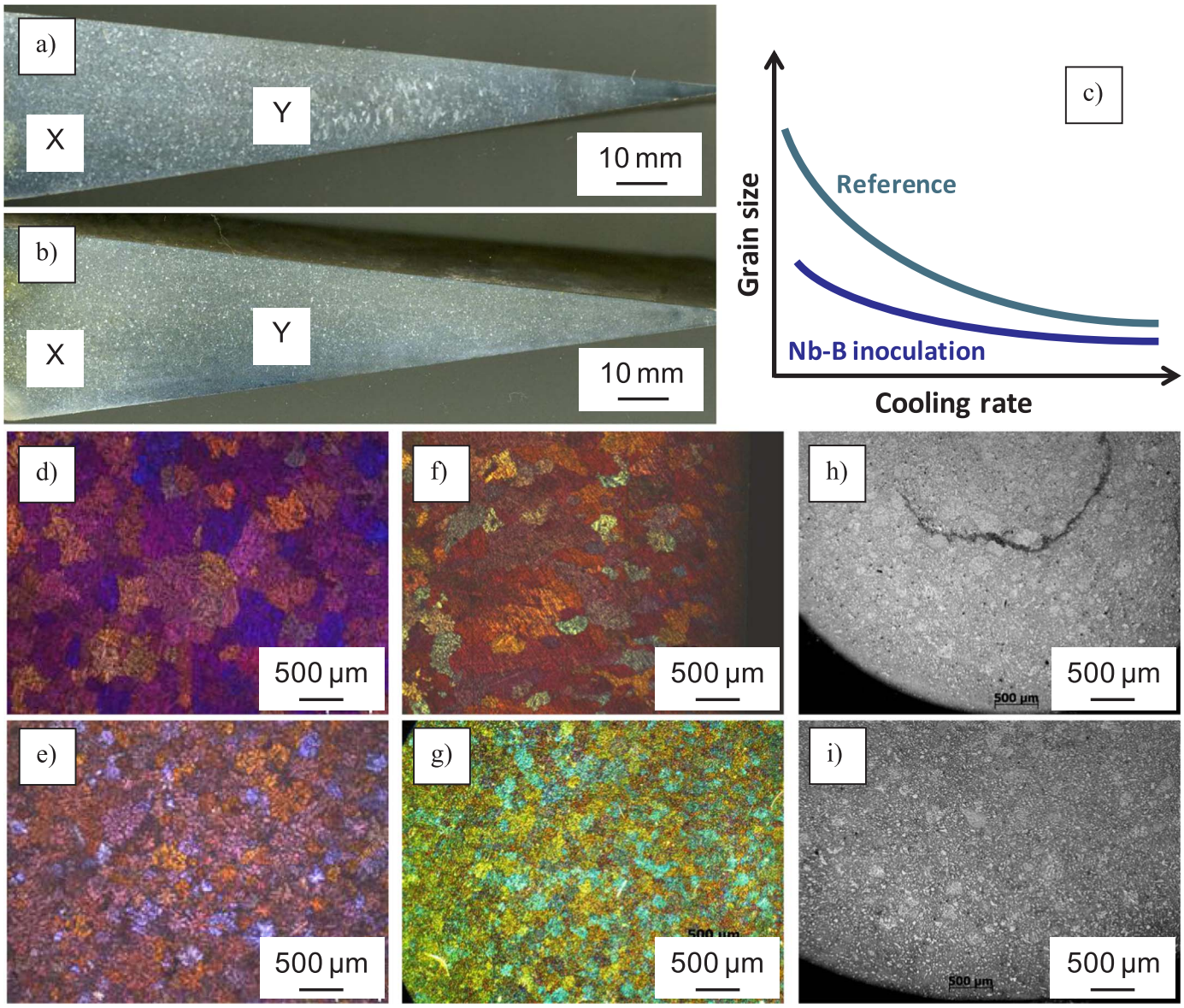

Fig. 2. Representative results of the microstructural characterisation of the AM50 alloy without and with Nb-B inoculation, respectively: a) and b) macroetched surfaces, c) sketch of the variation of the grain size, d) and e) micrographs at Pos. X, f) and g) micrographs at Pos. Y, and h) and i) micrographs of the HPDC samples.

As shown in Fig. 4, the Nb-B inoculation of the AM50 alloy results also in the improvement of the displacement to failure of flat (2 and 3 mm) samples in conjunction with the reduction of the variability of the data obtained. From Fig. 4(a), it can also be seen that, once again, the probability plot has a nearly linear trend. The consistent reduction of the scattering of the data, most of the times coupled with an enhancement of the property analysed, is an indication of the effectiveness of Nb-B inoculation in Al-containing Mg alloys.

3.3. Investigation on automotive components

Fig. 5 shows an example of the HPDC front end carrier industrial component used for the testing of the deflection to fracture of the AM50 alloy without and with Nb-B inoculation where it can be seen that the failure area of the front end carrier is located closed to the last filled region of the casting (i.e. Loc. 1). Out of the testing of a minimum of 13 HPDC parts it was found that the average deflection to failure was improved by 8.4% after Nb-B inoculation and there was not modification of the scatter of the data.

4. Discussion

Mg alloys have a great potential for the automotive industry to enable the weight saving needed to fulfil the every time stricter regulations about CO_2 emission. Mg has limited deformability (in comparison to its competitor metals) due to the few slip planes of the H.C.P. lattice [7]. Therefore, the manufacturing of components with appropriate mechanical performances by casting methods without any further downstream processing is very advantageous. The solidification of cast structures is controlled by the extraction of the latent heat of fusion from the solidification front and by the redistribution of the solute. Moreover, the solidification process itself is the outcome of the two contributing and competitive phenomena of formation of stable nuclei (i.e. nucleation) and their growth. The higher the cooling rate used to solidify the material the smaller the required critical nucleus for nucleation, the faster the extraction of the latent heat, and the shorter the time for grain growth. All of these aspects contribute to the reduction of the size of the grains composing the microstructure of the material and a decreasing trend is commonly obtained (Fig. 6). Specifically, the variation of the grain size (d) with the cooling rate (dT/dt) takes on a

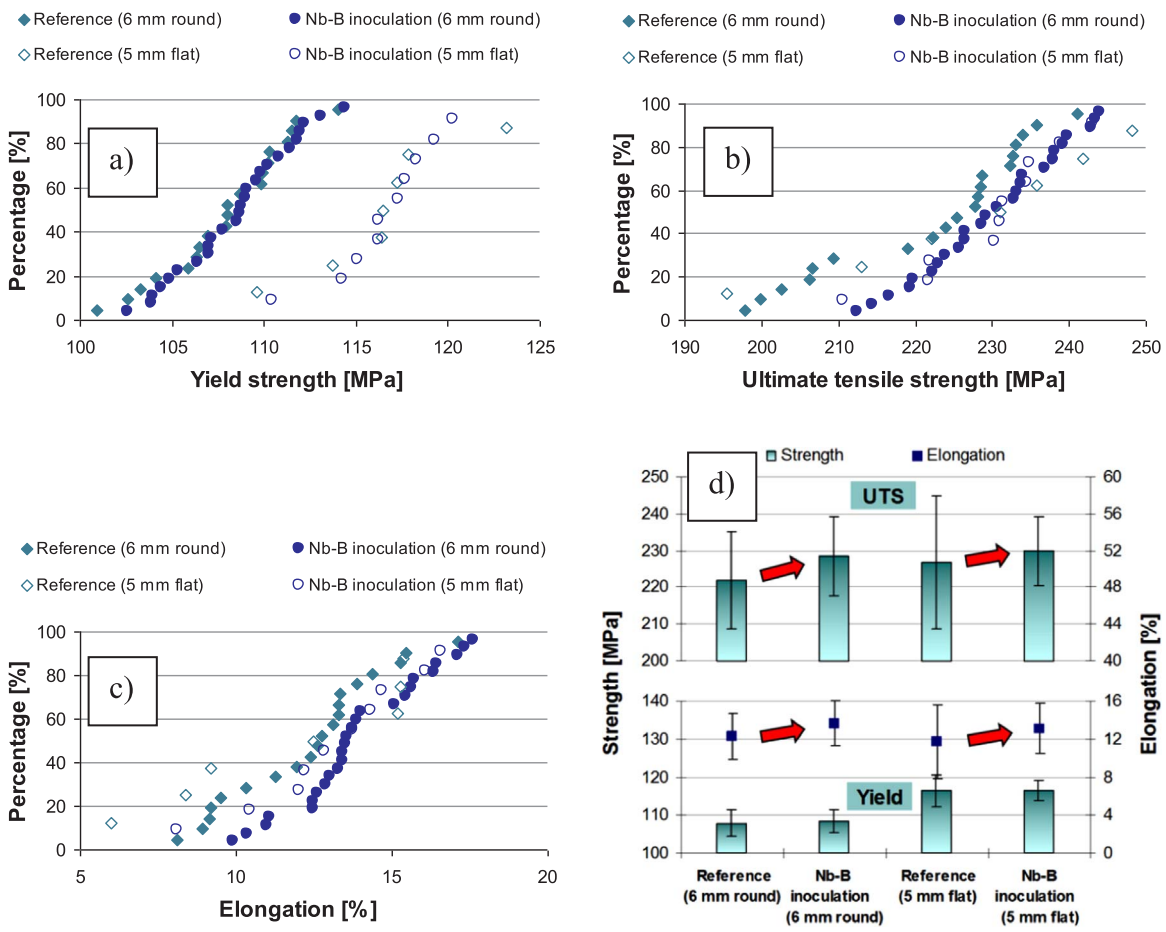

Fig. 3. Comparison of the tensile properties of the HPDC AM50 alloy samples without and with Nb-B inoculation: a) yield strength probability plot, b) ultimate tensile strength probability plot, c) elongation probability plot, and d) average tensile performances.

decreasing exponential distribution as the size of the equiaxed dendritic primary α-Mg crystals becomes coarser at very slow cooling rates such as in the case of sand casting where the solidification of the alloy takes place under a decrement of decimals of Celsius degrees per second.

The primary dendritic spacing λ_1 can be estimated via Eq. (1) [20] if the Gibbs-Thomson coefficient (Γ_{sl}), the diffusivity of the liquid phase (D_l), the equilibrium freezing range (ΔT_0), the partition coefficient (k_0), the growth velocity (v), and the temperature gradient (G) are available:

$$\lambda_1 = \left(-\frac{72\pi^2\Gamma_{sl}D_l\Delta T_0}{k_0}\right)^{1/4}(v)^{-1/4}(G)^{-1/2} \quad (1)$$

Most of these parameters are not-always-easy to quantify experimentally and appropriate empirical assumptions are normally made to use Eq. (1); it is worth noticing that $v{\cdot}G = dT/dt$ (i.e. the cooling rate employed to solidify the material). In the literature it has been proposed that in real casting situations Eq. (1) can be simplified into an exponential relationship between the measured grain size and the cooling rate as per Eq. (2) [21]:

$$d = d_0\ (\mathrm{dT/dt})^{-n} \quad (2)$$

where d_0 is the pre-exponential parameter that depends on the nature of the alloy studied and n is the exponential parameter [21]. From the inset in Fig. 6, Eq. (2) can successfully predict the grain size variation of cast Mg alloys where the trend is valid for both the AM50 alloy without

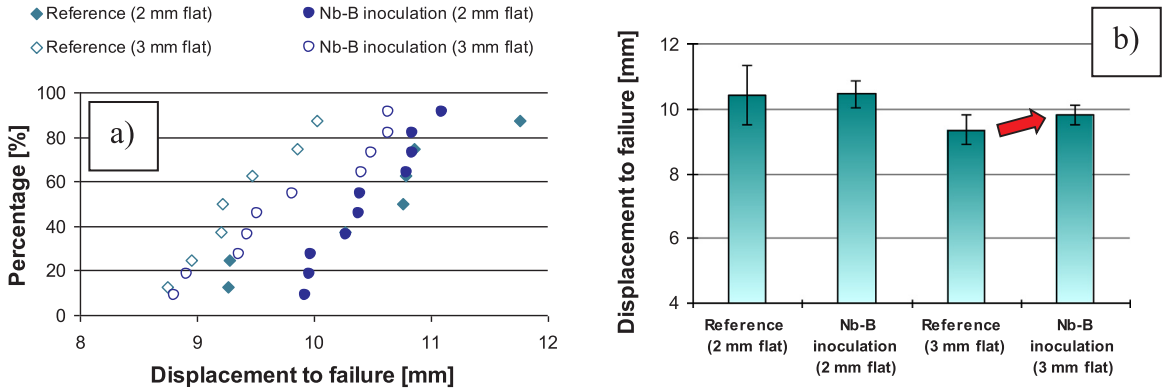

Fig. 4. Comparison of the bending properties of the HPDC AM50 alloy samples without and with Nb-B inoculation: a) displacement to fracture probability plot and b) average bending performances.

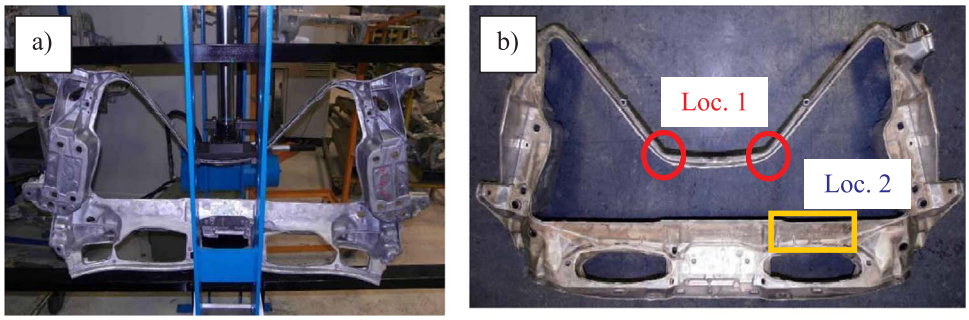

Fig. 5. AM50 alloy HPDC front end carrier industrial component used to test the deflection to failure: a) testing set-up and b) example of crashed component [31].

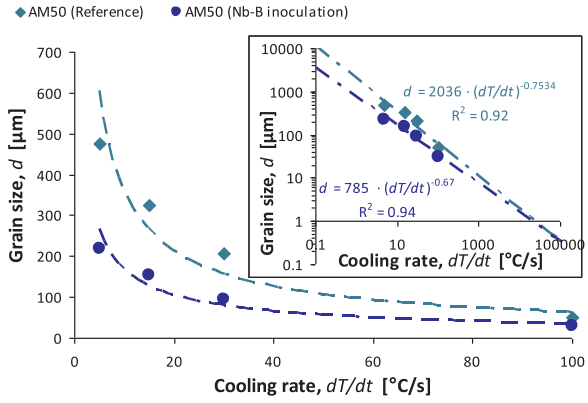

Fig. 6. Variation of the grain size of the AM50 alloy without (reference) and with Nb-B inoculation as a function of the cooling rate. Note: the prediction of the variation of the grain size as per Eq. (2) is shown as inset.

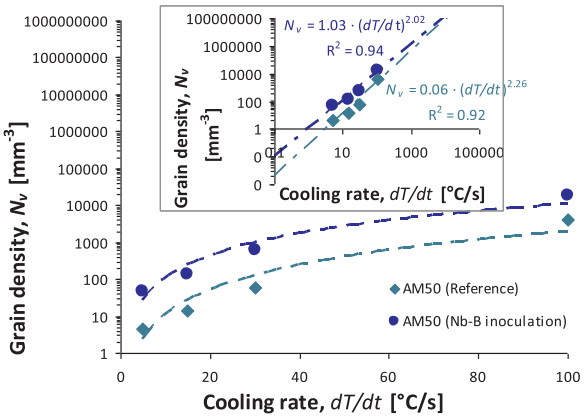

Fig. 7. Variation of the grain density of the AM50 alloy without (reference) and with Nb-B inoculation as a function of the cooling rate. Note: the prediction of the variation of the grain density as per Eq. (5) is shown as inset.

(reference) and with Nb-B inoculation. The introduction of stable heterogeneous nucleation sites with low lattice mismatch with the H.C.P. Mg hexagonal lattice boosts the nucleation step over the grain growth step of the overall solidification process. This results in a reduction of the final grain size and makes the variation of the size of the primary α-Mg dendrites less dependent on the actual cooling conditions. Solidification involves both nucleation and growth and once nucleation occurred it is generally assumed that equiaxed grains grow spherically. Under this assumption, the growth rate (V_s) depends on the radius of the grains (R_g), the diffusivity (D), and the parameter (λ_s) as per the growth kinetic model proposed by Maxwell and Hellawell [22]:

$$V_s = \frac{\lambda_s^2 \cdot D}{2R_g} \tag{3}$$

As nucleation is completed and only further growth of the grains present takes place, a maximum number of grains per unit volume (i.e. grain density, N_v) is obtained. It is normally supposed that a real cast structure has a log-normally distribution of grains and therefore the relationship proposed by Greer et al. [23] applies:

$$d = \sqrt[3]{\frac{0.5}{N_v}} \tag{4}$$

Fig. 7 shows the calculated relationship between the cooling rate and the grain density of the AM50 alloy solidified without and with inoculation where both materials show an exponential trend as solidification is governed by thermal gradient and growth velocity. In a similar manner to the grain size, the variation of the grain density with the cooling rate can be simplified into an exponential relationship, Eq. (5):

$$N_v = N_{v0} \ (dT/dt)^{-m} \tag{5}$$

The result of the analysis of the experimental data using Eq. (5) is reported as inset in Fig. 7. In this case the pre-exponential parameter (N_{v0}) and the exponential parameter (m) are also related to the nature of the alloy considered. As in this study the major difference between the two alloy systems is inoculation, the trend gives an estimation of its relative influence. Inoculation has its greatest effect at slow cooling rates and becomes less predominant as the time for solidification is reduced. The volumetric grain density of the inoculated alloy is more than 30 times higher than that of the reference material for a cooling rate of 0.1 °C/s (e.g. sand casting) and only slightly higher (i.e. 0.05%) at 10^6 °C/s, typical of atomisation processes. The ratio between the pre-exponential parameter (N_{v0}) of the inoculated alloy and that of the reference material (i.e. 17.4) also provides an estimation of the potency of the heterogeneous substrates added to promote nucleation. It is worth to note that in the case of the reference material the grain density approaches zero as the system moves towards equilibrium solidification conditions. At very slow cooling rate the volumetric grain density tends to zero predicting the material to be composed of very few coarse grains and this is actually found in practical casting instances.

The efficacy of intentionally introduced heterogeneous nucleation substrates is related to the undercooling (ΔT), which in turns is related to the lattice mismatch (f) [24]. Thus, the higher the efficacy of the heterogeneous substrates the finer the grain size of the material. A rigorous analysis of the nucleation process should consider the impact of the free energy at the nucleating interface but this is not normally performed because of the difficulty on quantifying many of the contributing factors. Alternatively, a model based on the interatomic distance along low index crystallographic planes between the substrate and the nucleating phase was proposed by Bramfitt [25]. Under the assumption that the energy barrier for heterogeneous nucleation is purely dependent on structural aspects of the nucleating phase/substrate interface, this energy reaches its minimum value for coherent interfaces, which give the lowest possible energy barrier. The lattice mismatch is then calculated as per Eq. (6) [26]:

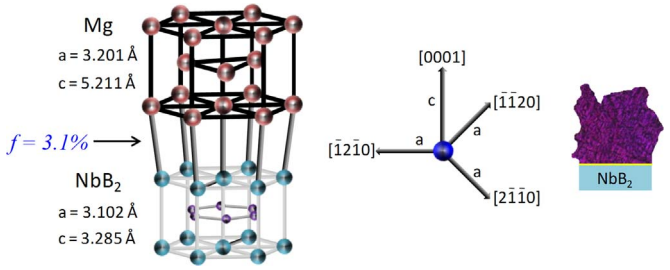

Fig. 8. Sketch of the Mg and Nb_2 hexagonal close-packed lattice structure where the lattice mismatch (f) along their (0001) basal plane is highlighted.

$$f = \Delta a / a_0 \quad (6)$$

where Δa is the mean difference in lattice parameters along low index planes between the substrate and the nucleating phase and a_0 is the lattice parameter of the solidifying material (i.e. primary α-Mg in this study) [24,25]. The enhancement of the solidification of Al-containing Mg alloys can be achieved with the intentional introduction of potent heterogeneous nucleation substrates. In the case of Nb-B inoculation via Al-Nb-B master alloy, Nb-based compounds and, in particular, NbB_2 intermetallics are the particles responsible to favour and improve the nucleation stage over the growth of the grain as we previously reported on a preliminary work about the AZ91 alloy [27]. Specifically, NbB_2 and Mg are isomorphous and have comparable lattice parameter: a = 3.102 Å and c = 3.285 Å for NbB_2 and a = 3.201 Å and c = 5.211 Å for Mg, respectively. The lattice mismatch along the (0001) basal plane between these two structures is 3.1% as schematically shown in Fig. 8. It is worth mentioning that Mg- and Al-boride particles could also be formed when the Al-Nb-B master alloy is dissolved into the Mg alloys. Nevertheless, this is less thermodynamically favourable on the base of the enthalpy of formation of these compounds [28–30].

Cold chamber HPDC is a peculiar casting process because the material is injected into the mould cavities and, therefore, undergoes high shear rates and significantly fast cooling. There is an important initial solidification occurring over a time-scale of milliseconds, leading to non-equilibrium conditions and microstructures are very different to those observed in other casting methods. Initially, there is growth of primary α-Mg dendrites in the shot sleeve before injection of the melt into the die and, thus, the material injected is, in fact, a partially solidified alloy. The central region of the HPDC product may be predominantly formed by segregation and agglomeration of primary crystals which were formed in the shot sleeve before injection into the die. The liquid, which is richer in solute, segregates to regions closer to the die walls. During filling and the short feeding stage, the microstructure develops in response to the high flow rates. Solidification begins as soon as the molten metal reaches the relatively cold mould walls. This results in a very fine microstructure and a high volume fraction of non-equilibrium eutectic phases such as β-$Mg_{17}Al_{12}$ found close to the mould walls. The HPDC solidified structure as well as its properties can be assimilated to that of a composite material [31]. The outer material, known as skin, is homogeneous all over the cast part and so the consistency of the mechanical properties; however, the core of the material is rather uniform near the injection gate but this uniformity is lost as the distance from the injection point increases. This leads to a decrement of the mean properties and significantly increases the scatter of the data. This effect is already present in lab scale components, as visible in Figs. 3 and 4, and it is amplified in large structural parts manufactured by HPDC. That is why the design of these HPDC large structural components is commonly done in a conservative way and the reduction of the uncertainty is a key factor. The conservative design approach is paramount in order to ensure the performance of the HPDC part even when the stressed or loaded area is located far away from the injection gate. The Nb-B inoculation of the AM50 alloy helps in reducing the scattering of the data and leads to the improvement of the mechanical performance, especially in terms of ductility and elongation. In the case of the strength, both yield and ultimate tensile, the enhancement is rather limited in the case of HPDC samples because the grain size of the reference material is already fine (~ 40 μm). The improvement is due to the refinement of the grain size down to roughly 30 μm induced by the inoculation. The grain size of the microstructure

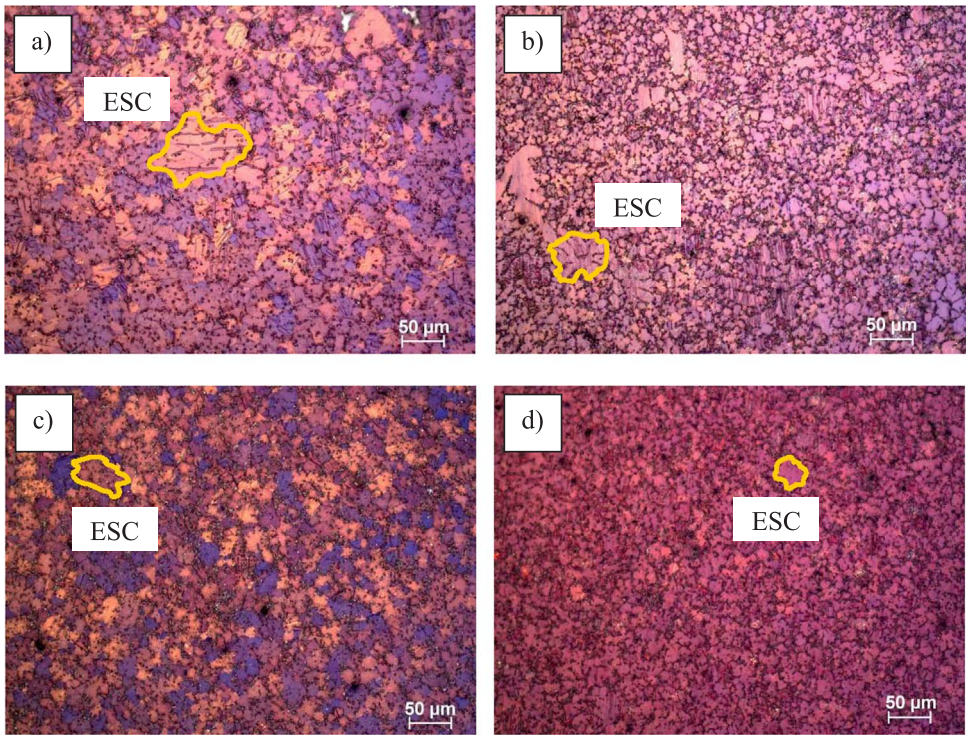

Fig. 9. Optical micrographs of the AM50 alloy components shown in Fig. 5: a) reference – Loc. 1, b) reference – Loc. 2, c) Nb-B inoculation – Loc. 1 and d) Nb-B inoculation – Loc. 2. Note: ESCs – early solidified crystals.

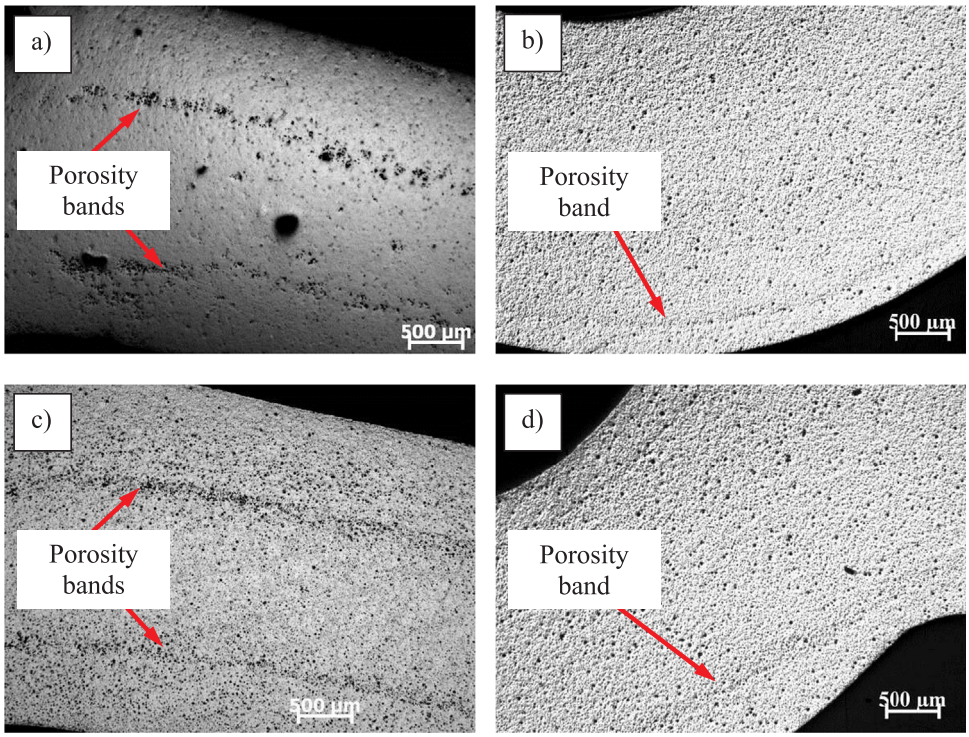

Fig. 10. Optical micrographs of the defect bands found in AM50 alloy components shown in Fig. 5: a) reference – Loc. 1, b) reference – Loc. 2, c) Nb-B inoculation – Loc. 1 and d) Nb-B inoculation – Loc. 2.

of the front end carrier HPDC AM50 alloy is shown with the aim of the micrographs reported in Fig. 9 which were taken at Loc. 1 and Loc. 2 shown in Fig. 5.

It can be seen that, apart from dendritic primary α-Mg crystals, the microstructure of the HPDC reference AM50 alloy is characterised by the presence of some coarse grains in the range of 150 µm (Fig. 9(a) and (b)). These sort of grains are typical of the HPDC process and are known as early solidified crystals (ESCs) because they form when the molten alloy is poured inside in the (much colder) shot sleeve for injection. Al-containing Mg alloys are sensitive to the formation of ESCs which, actually, leads to loss of the mechanical performances and scattering of the data [32]. Nb-B inoculation does not only refine the microstructure but also reduces the mean size of ESCs down to approximately 70 µm as it can be seen in Fig. 9(c) and (d). Another particularity of the structure of HPDC components is the formation of defect bands (porosity and/or segregation) which can be seen in the micrographs shown in Fig. 10 which were taken at Loc. 1 and Loc. 2 shown in Fig. 5. Porosity bands were also present in the AM50 reference HPDC round tensile samples (Fig. 2(h)) but not in the Nb-B inoculated alloy (Fig. 2(i)).

In the case of the reference material, the defect bands are very pronounced in Loc. 1 (Fig. 10(a)) whereas are hardly visible in Loc. 2 (Fig. 10(b)). The actual amount of solidification taking place during the formation of these bands combined with the deformation induced by the shear of the flowing melt are the responsible for the formation of these bands. Two opposite scenarios are possible depending whether significant or very little solidification takes place before the shooting. Defect bands (Fig. 10(a)) are formed when significant solidification occurs whilst segregation bands (Fig. 10(b)) appears if the mould is rapidly filled without much early solidification. The total quantity of porosity in the band also increases if there is not sufficient liquid metal to flow between the interdendritic network [32]. From the micrographs of Fig. 10, it can be seen that Nb-B inoculation changes the nature of the defect bands although its effect is much more visible and pronounced in Loc. 1 (Fig. 10(c)) which is, actually, located away from the injection gate. Specifically, a much narrower distribution of smaller pores is obtained instead of the coarse structure found in the reference alloy. Therefore, in the case of HPDC structure, beside the refinement of the microstructure, the most striking feature of Nb-B inoculation is the ability to modify the porosity bands. The size and distribution of ESCs and the characteristics of the defect bands present in the HPDC parts are the responsible for the variation of the mechanical performances as a function of the thickness and shape of the samples (Figs. 3 and 4). Nb-B inoculation leads to a gain in performances, especially elongation, as a consequence of the enhancement on local solidification and formation of porosity and this is further proven by the enhanced deflection found in automotive HPDC components (Fig. 5).

The Hall-Petch plot where the strength of the AM50 produced by different casting processes such as gravity die casting (GDC) [33], low pressure die casting (LPDC) [33], permanent mould casting (PMC) [34], and HPDC versus the grain size are analysed is presented in Fig. 11(a). For the sake of comparison, the behaviour of pure Mg is also shown [35] to highlight the effect of the alloying elements. The presence of Al and Mn intrinsically increases the stress needed for dislocation movement σ_o, which is a material-dependent constant, from 14.0 MPa to 31.3 MPa and the strengthening coefficient k. The strength of the AM50 alloy increases with the decrement of the grain size or, in turns, with the increment of the cooling rate used to solidify the alloy.

Data from Peng et al. [33] and Neh et al. [34] were used to estimate the variation of the mechanical properties (yield strength, ultimate tensile strength and elongation) with the grain size (i.e. straight lines in Fig. 11(b)) and, therefore, to predict the mechanical behaviour depending on the cooling conditions (Fig. 6). It is worth mentioning that the data and the prediction for the HPDC process were not considered because for this method the properties are highly affected by the formation of a non-equilibrium microstructure composed of a high number of eutectic compounds, defect bands and segregation bands as previously discussed. The actual improvement achievable by grain refinement is directly related to the variation of each specific properties with the grain size and it ranges from 3.2% up to 33% depending on the process and the associated inherent cooling rate.

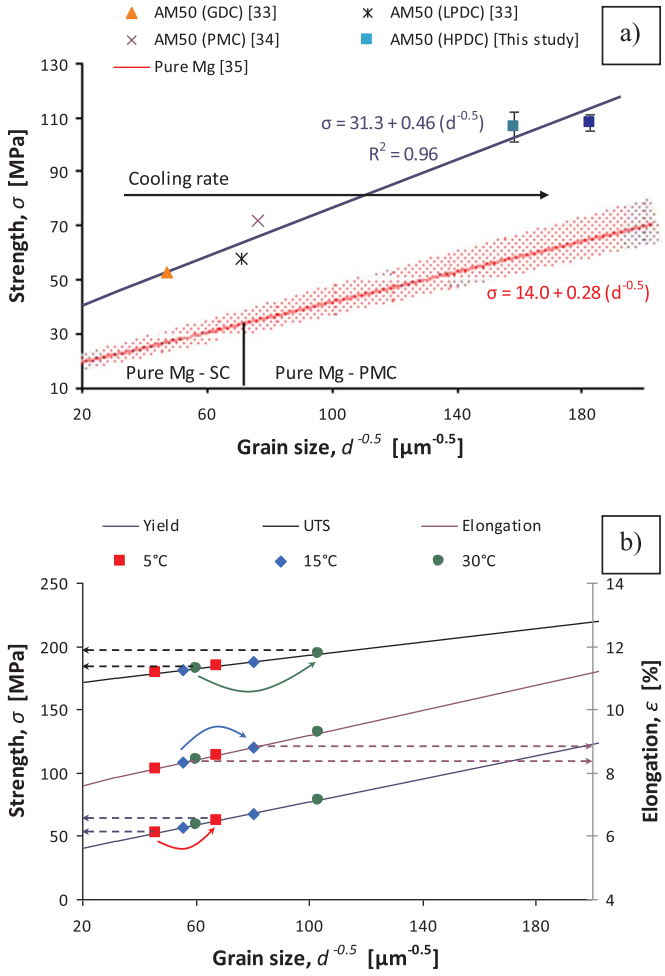

Fig. 11. Hall-Petch plots for the AM50 alloy processed by different casting processes: a) yield strength vs grain size; pure Mg is also shown for comparison, and b) prediction of the mechanical properties of the AM50 alloy for the equilibrium cooling conditions shown in Fig. 6. Legend – GDC: gravity die casting, LPDC: low pressure die casting, PMC: permanent mould die casting, HPDC: high pressure die casting and SC: sand casting.

5. Conclusions

On the basis of the discussion presented we conclude that Nb-B inoculation of Al-containing Mg alloys, done by means of the addition of Al-Nb-B master alloys, promotes the nucleation stage of primary α-Mg dendritic grains over their growth. The enhanced nucleation results in the refinement of the α-Mg grains composing the solidified alloy where this grain refinement is obtained throughout a great range of cooling rates. The most significant refinement is achieved at low cooling rates where the improving of nucleation is much more needed. We also demonstrate that the refinement of the grain structure corresponds to increased mechanical performances. In the case of cold chamber high pressure die casting products where the grain size is already very fine due to the extremely fast cooling conditions, Nb-B inoculation helps to reduce the variability of the strength and makes the Mg alloys more ductile. The increment of the ductility is due to both reduction of the grain size and reduction of the defect or porosity bands present in the cold chamber high pressure die casting components. As per the Hall-Petch relationship, a greater improvement of the strength and a more consistent response for Al-containing Mg alloys is expected when they are processed with casting methods characterised by lower cooling rates like die casting or sand casting where the refining effect of Nb-B inoculation is much more pronounced.

Data availability

All metadata pertaining to this work can be accessed via the following link: https://10.17633/rd.brunel.595217.

Acknowledgements

The financial support from Engineering and Physical Sciences Research Council (EPSRC) through the EP/J013749/1 and EP/K031422/1 Projects as well as from the Technology Strategy Board (TSB) through the TSB/101177 Project are acknowledged.

References

[1] E. Volkova, Modern magnesium-based deformable alloys and composite materials (a review), Met Sci. Heat Treat. 48 (2006) 473–478.
[2] I.J. Polmear, Light Alloys from Traditional Alloys to Nanocrystals, 4th ed., Butterworth-Heinemann, UK, 2006.
[3] A.K. Dahle, D.H. St. John, G.L. Dunlop, Developments and challenges in the utilisation of magnesium alloys, Mater. Sci. Forum 24 (2000) 167–182.
[4] A.A. Luo, Recent magnesium alloy development for elevated temperature applications, Int. Mater. Rev. 49 (2004) 13–30.
[5] M. Kulekci, Magnesium and its alloys applications in automotive industry, Int. J. Adv. Manuf. Technol. 39 (2008) 851–865.
[6] J. Du, M. Wang, W. Li, Effects of Fe addition and addition sequence on carbon inoculation of Mg-3%Al alloy, J. Alloy. Compd. 502 (2010) 74–79.
[7] S.J. Liang, Z.Y. Liu, E.D. Wang, Microstructure and mechanical properties of Mg-Al-Zn alloy deformed by cold extrusion, Mater. Lett. 62 (2008) 3051–3054.
[8] M.A. Jabbari-Taleghani, J.M. Torralba, Hot workability of nanocrystalline AZ91 magnesium alloy, J. Alloy. Compd. 595 (2014) 1–7.
[9] S.W. Xu, S. Kamado, N. Matsumoto, T. Honna, Y. Kojima, Recrystallization mechanism of As-cast AZ91 magnesium alloy during hot compressive deformation, Mater. Sci. Eng. A 527 (2009) 52–60.
[10] E.F. Emley, Principles of Magnesium Technology, Pergamon Press, Oxford, 1966.
[11] D.H. St. John, M. Qian, M. Easton, P. Cao, Z. Hildebrand, Grain refinement of magnesium alloys, Metall. Mater. Trans. A 36 (2005) 1669–1679.
[12] Y.C. Lee, A.K. Dahle, D.H. St. John, The role of solute in grain refinement of magnesium, Metall. Mater. Trans. A 31 (2000) 2895–2906.
[13] Y. Ali, D. Qiu, B. Jiang, F. Pan, M.-X. Zhang, Current research progress in grain refinement of cast magnesium alloys: a review article, J. Alloy. Compd. 619 (2015) 639–651.
[14] Z.H. Gu, I.Y. Wang, N. Zheng, M. Zha, L.L. Jiang, W. Wang, G.Q. Jiang, Effect of melt superheating treatment on the cast microstructure of Mg-1.5Si-1Zn alloy, J. Mater. Sci. 43 (2008) 980–984.
Farbenindustrie, 1931 [15] I.G. Farbenindustrie, British Patent GB359, 425, 1931.
[16] S.F. Liu, L.Y. Liu, L.G. Kang, Refinement role of electromagnetic stirring and strontium in AZ91 magnesium alloy, J. Alloy. Compd. 450 (2008) 546–550.
[17] G. Wu, Y. Fan, H. Gao, C. Zhai, Y.P. Zhu, The effect of Ca and rare earth elements on the microstructure, mechanical properties and corrosion behavior of AZ91D, Mater. Sci. Eng. A 408 (2005) 255–263.
[18] M. Nowak, W.K. Yeoh, L. Bolzoni, N. Hari Babu, Development of Al-Nb-B master alloys using Nb and KBF_4 powders, Mater. Des. 75 (2015) 40–46.
[19] L. Bolzoni, M. Xia, N. Hari Babu, Formation of equiaxed crystal structures in directionally solidified Al-Si alloys using Nb-based heterogeneous nuclei, Sci. Rep. 6 (2016) 39554.
[20] J.A. Dantzig, M. Rappaz, Solidification, EPFL Press, Switzerland, 2009, p. 324.
[21] M.C. Flemings, Solidification processing, Metall. Mater. Trans. B 5 (1974) 2121–2134.
[22] I. Maxwell, A. Hellawell, A simple model for refinement during solidification, Acta Metall. 23 (1975) 229–237.
[23] A.L. Greer, A.M. Bunn, A. Tronche, P.V. Evans, D.J. Bristow, Modelling of inoculation of metallic melts: application to grain refinement of aluminium by Al-Ti-B, Acta Mater. 48 (2000) 2823–2835.
[24] D. Turnbull, B. Vonnegut, Nucleation catalysis, Ind. Eng. Chem. 44 (1952) 1292–1298.
[25] B.L. Bramfitt, The effect of carbide and nitride additions on the heterogeneous nucleation behavior of liquid iron, Metall. Mater. Trans. B 1 (1970) 1987–1995.
[26] J.E. Burke, D. Turnbull, Recrystallization and grain growth, Prog. Met. Phys. 3 (1952) 220–292.
[27] L. Bolzoni, M. Nowak, N. Hari Babu, Nb-based heterogeneous nuclei for enhanced α-Mg nucleation in Mg(-Al) alloys, Mater. Lett. 169 (2016) 207–209.
[28] H.-Y. Wang, W. Wang, M. Zha, N. Zheng, Z.-H. Gu, D. Li, Q.-C. Jiang, Influence of the amount of KBF_4 on the morphology of Mg_2Si in Mg-5Si alloys, Mater. Chem. Phys. 108 (2008) 353–358.
[29] I. Barin, Thermochemical Data of Pure Substances, VCH Verlagsgesellschaft mbH, Weinheim, Germany, 1993.
[30] F. Zhao, X. Xing, C. Xiao, R. Hu, L. Xue, H. Gao, L. Xiao, T. An, Study on thermodynamics and kinetics for the reaction of magnesium diboride and water by microcalorimetry, Am. J. Anal. Chem. 2 (2011) 270–275.
[31] R. Alain, T. Lawson, P. Katool, G. Wang, L. Jekl, R. Berkmortel, L. Miller, J. Svalestuen, H. Westengen, Robustness of Large Thin Wall Magnesium Die Castings

for Crash Applications, SAE Technical Paper, 2004-01-0131, 2004.
[32] H.I. Laukli, High Pressure Die Casting of Aluminium and Magnesium Alloys, Grain Structure and Segregation Characteristics, Department of Materials Science and Engineering, NTNU, Trondheim, 2004. Available at: ⟨http://brage.bibsys.no/xmlui/handle/11250/248738⟩.
[33] L.M. Peng, P.H. Fu, H.Y. Jiang, C.Q. Zhai, Microstructure and mechanical properties of low pressure die cast AM50 magnesium alloy, Mater. Sci. Forum 546–549 (2007) 167–170.
[34] K. Neh, M. Ullmann, R. Kawalla, Effect of grain refining additives on microstructure and mechanical properties of the commercial available magnesium alloys AZ31 and AM50, Mater. Today: Proc. 2 (2015) S219–S224.
[35] C.H. Caceres, G.E. Mann, J.R. Griffiths, Grain size hardening in Mg and Mg-Zn solid solutions, Metall. Mater. Trans. A 42 (2011) 1950–1959.